Nitrogen-Doped Graphene and Its Application in Electrochemical Biosensing

Ying Wang,[†,‡] Yuyan Shao,[‡] Dean W. Matson,[‡] Jinghong Li,[†,*] and Yuehe Lin[‡,*]

[†]Department of Chemistry, Key Laboratory of Bioorganic Phosphorus Chemistry & Chemical Biology, Tsinghua University, Beijing 100084, People's Republic of China, and [‡]Pacific Northwest National Laboratory, Richland, Washington 99352

ABSTRACT Chemical doping with foreign atoms is an effective method to intrinsically modify the properties of host materials. Among them, nitrogen doping plays a critical role in regulating the electronic properties of carbon materials. Recently, graphene, as a true two-dimensional carbon material, has shown fascinating applications in bioelectronics and biosensors. In this paper, we report a facile strategy to prepare N-doped graphene by using nitrogen plasma treatment of graphene synthesized *via* a chemical method. Meanwhile, a possible schematic diagram has been proposed to detail the structure of N-doped graphene. By controlling the exposure time, the N percentage in host graphene can be regulated, ranging from 0.11 to 1.35%. Moreover, the as-prepared N-doped graphene has displayed high electrocatalytic activity for reduction of hydrogen peroxide and fast direct electron transfer kinetics for glucose oxidase. The N-doped graphene has further been used for glucose biosensing with concentrations as low as 0.01 mM in the presence of interferences.

*Address correspondence to yuehe.lin@pnl.gov, jhli@mail.tsinghua.edu.cn.

Graphene, emerging as a true two-dimensional material, has shown its fascinating applications in bio-electronics and biosensing.[1,2] Applications include a graphene-based single bacterium device or DNA transistor,[3] glutathione detection with graphene oxide enhanced electrochemiluminescence,[4] a biosensing platform of chemically reduced graphene,[5] and glucose biosensing on a graphene/ionic liquid interface.[6] Due to the unique physical and chemical properties of graphene, such as high surface area, excellent conductivity, ease of functionalization and production, graphene provides an ideal base for electronics, electric devices, and biosensors.[7−9] Hence, tailoring and developing the electronic characteristics of graphene to achieve unique properties has attracted great attention recently.[10−12] Specifically, electronic properties of graphene have been altered by chemical functionalization[13] and electrochemical modification.[14] Meanwhile, numerous hybrids such as graphene/polymer nanocomposites,[15] graphene/Pt nanoparticle sheets,[16] and graphene/metal oxide deposits[17] have been reported. However, most of these approaches have been aimed at producing graphene hybrids with synergy or multiple functionalities. Little attention has been paid to intrinsic modification of graphene with the purpose of enhancing the graphene performance in bioelectrochemical systems.

Chemical doping with foreign atoms is an effective method to modify materials intrinsically, tailor electronic properties, manipulate surface chemistry, and produce local changes to the elemental composition of host materials.[18,19] For carbon materials, chemical doping is also a leading potential strategy to enrich free charge-carrier densities and enhance the electrical or thermal conductivities.[20,21] Recent studies have demonstrated efforts at chemical doping of graphene.[22,23] For example, by using an oxygen etching process, graphene is simultaneously etched and surface doped by oxidation.[24] Theoretical investigation of metal-doped graphene has predicted the possibility of a Fermi level shift and a crossover from p-type to n-type.[25] Among the numerous potential dopants, nitrogen is considered to be an excellent element for the chemical doping of carbon materials because it is of comparable atomic size and contains five valence electrons available to form strong valence bonds with carbon atoms.[26] In previous work, N doping has been successfully employed to modify the electrical or structural properties of carbon nanotubes (CNTs). For instance, N doping of CNTs increases the metallic behavior,[27] affects the lattice alignment,[28] and regulates the growth mechanism.[29] Moreover, it has been demonstrated that N doping enhanced the biocompatibility and sensitivity of CNTs in biosensing applications.[30,31]
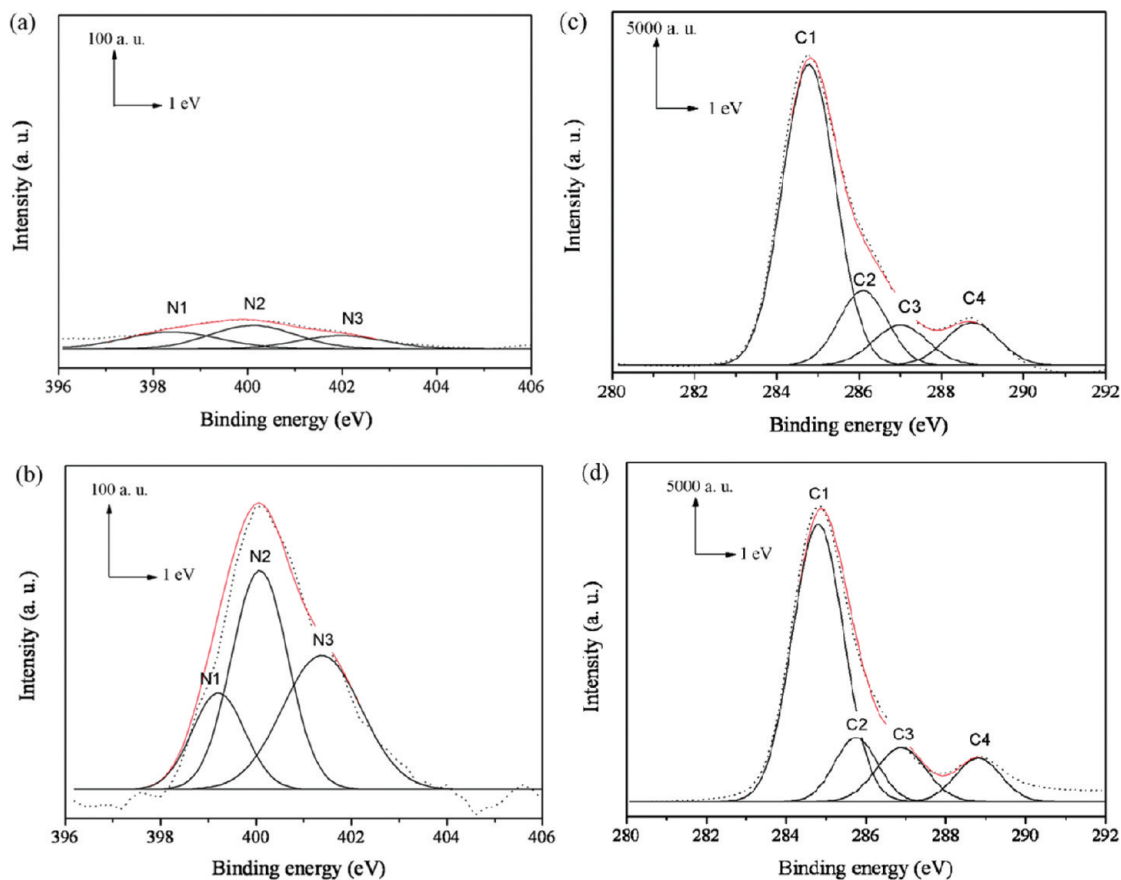
Figure 1. XPS N_{1s} spectra of graphene (a) and N-doped graphene (b) with N1 (pyridinic N), N2 (pyrrolic N), and N3 (quaternary N); C_{1s} spectra of graphene (c) and N-doped graphene (d) with C1 (C−C), C2 (C−O), C3 (C═O or C−N), and C4 (C−C═O).

Consequently, N doping has great potential to be used for graphene modification. So far, only a few studies have been aimed at producing N-doped graphene *via* electrothermal reaction with ammonia[32] or chemical vapor deposition.[33]

In this paper, we report a strategy to synthesize N-doped graphene through nitrogen plasma treatment of graphene and further investigate application of the doped graphene in electrocatalysis and biosensing applications. Plasma treatment is a simple approach for material surface modification and could be used for the introduction of foreign atoms, groups, or structures onto bulk scaffold surfaces.[34] Graphene used in the current work was prepared by a chemical method based on the Hummers and Offeman oxidation[35] (see our previous works related to the synthesis and characterization of graphene[36,37]). After doping by plasma treatment, the structure of N-doped graphene is further proposed to show the N status in graphene carbon layers and detail the possible active sites or defects based on X-ray photoelectron spectroscopy (XPS) studies of the modified material. By controlling plasma exposure time, the percentage of nitrogen doping could be regulated and optimized easily. Furthermore, N-doped graphene was successfully applied for electrocatalysis and biosensing. The reduction potential of

H_2O_2 at N-doped graphene electrode shifted 400 mV positively with ~20 times current enhancement compared with a glassy carbon electrode. Additionally, N-doped graphene showed excellent biocompatibility and fast electron transfer kinetics for glucose biosensing to concentrations as low as 0.01 mM in the presence of interferences.

RESULTS AND DISCUSSION

Synthesis and Microstructure of N-Doped Graphene. Nitrogen-doped graphene was fabricated by N plasma treatment of graphene that was chemically synthesized based on the Hummers and Offeman method[35] with some optimizations according to our previous work.[36,37] Graphene was dispersed in chitosan (0.5 wt % with 2% acetic acid) with sonication to form a 1 mg mL^{-1} graphene−chitosan dispersion. Five microliters of graphene−chitosan solution was coated on the surface of a glassy carbon electrode (GCE). After drying, graphene was firmly attached onto the GCE surface because of the hydrophobic interface between graphene and glassy carbon with chitosan immobilization. The graphene−chitosan/GCE was placed in a plasma chamber which was backfilled with a nitrogen atmosphere at a pressure of 750 mTorr. Plasma power was 100 W,

TABLE 1. Atomic Concentration of C, N, and O of Chemically Synthesized Graphene and N-Doped Graphene[a]

sample	area	C_{1s} (%)	N_{1s} (%)	O_{1s} (%)
graphene	1	84.26	0.18	15.56
	2	85.53	0.11	14.36
N-doped graphene	1	71.09	1.35	28.05
	2	72.77	1.26	26.54

[a]Nitrogen doping was achieved by nitrogen plasma treatment for 40 min in the chamber with the pressure of 750 mTorr and the power of 100 W. Two different areas of each sample were tested and shown with the percentage of each element.

and treatment time was controlled from 20 to 100 min to obtain various N doping percentages.

XPS is a powerful tool to identify the elements' states in bulk material.[38] By analysis of binding energy (BE) values, we can confirm the nature of the binding between carbon and nitrogen. Core-level high-resolution XPS spectra in the N_{1s} binding energy range was obtained on N-doped graphene and graphene. As shown in Figure 1a, no obvious distinct N peaks are observed for graphene. However, nitrogen peaks in the spectra of N-doped graphene were observed at BE = 398.9 eV for pyridinic N, BE = 400.1 eV for pyrrolic N, and BE = 401.5 eV for quaternary N (Figure 1b).[39−41] Table 1 shows the atomic percentage of nitrogen, carbon, and oxygen in graphene and N-doped graphene. Chemical reduction of graphene oxide with hydrazine introduced trace N (0.145%) into graphene. After the plasma treatment, N percentage increased up to 1.35%, indicating the successful doping of nitrogen. XPS of C_{1s} ranging from 282 to 290 eV is shown as Figure 1c,d. Generally, there are several different C groups in chemically synthesized graphene, which are characterized by the appearance of several spectral peaks: C−C at 284.8 eV, C−OH at 285.9 eV, C═O at 287.1 eV, and C−C═O at 289.0 eV (Figure 1c). As is well-known, the peak of C═O is overlaid with C−N around the binding energy of 287.5 ± 0.5 eV.[42,43] As shown in Figure 1d, the peak at 287.1 eV for C═O or C−N increased obviously after N doping. It also demonstrated successful doping of N into the graphitic layer of graphene. The intensity peaks

characteristic of the C−O groups increased, but those characteristics of C−C decreased, indicating that doping not only introduced nitrogen atoms into host graphene but also increased the content of oxygen. Meanwhile, plasma treatment might change the natural structure of functional oxygen groups in graphene. XPS spectra of O_{1s} before and after N doping are shown as Figure 2 (C−OH at 533.9 eV, C═O at 532.5 eV, and C(O)OH at 531.8 eV[44]). After the doping, oxygen content was found to have increased to 27.5 at %.

Figure 3 shows the transmission electron microscope (TEM) images of chemically synthesized graphene (Figure 3a) and N-doped graphene (Figure 3b). As can been seen from Figure 3, the graphene planar sheets are observed clearly in N-doped graphene, indicating that the features of high surface/volume ratio and two-dimensional structure of graphene morphology are well maintained. A schematic diagram of the effect of nitrogen doping on the graphene structure is displayed as Scheme 1, showing the possible N locations in N-doped graphene. According to XPS results, three types of doping N, including pyridinic N, pyrrolic N, and quaternary N, could be formed. Each type is characterized by a specific binding energy shown in XPS spectra: 398.9 eV for pyridinic N, 400.1 eV for pyrrolic N, and 401.5 eV for quaternary N. Such doped N atoms would decorate the graphene planar sheet and introduce a change in the Fermi level, engendering the doping effects and opening the band gap of the graphene.[24] Therefore, N doping might play an important role in regulating the electronic properties and enhancing the electrocatalytic activity of graphene in electrochemical systems.

Electrocatalysis of N-Doped Graphene. To explore the application of N-doped graphene in electrochemistry, cyclic voltammetric characteristics of H_2O_2 at a N-doped graphene electrode were investigated. H_2O_2 is an important regulator of eukaryotic signal transduction, generated in response to various stimuli including cytokines and growth factors.[45] As shown in Figure 4a, the GCE showed a weak response to 5 mM H_2O_2 at −0.59 V in nitrogen-
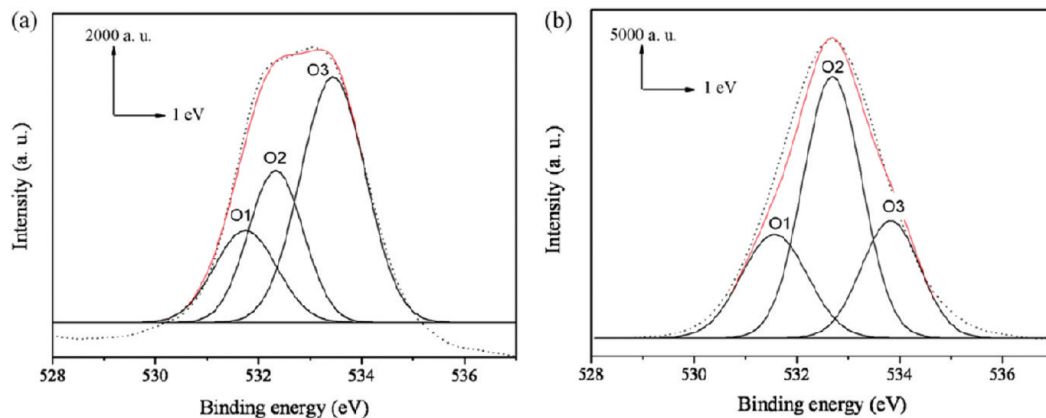

Figure 2. (a) XPS O_{1s} spectra of graphene (a) and N-doped graphene (b) with O1 (HO−C═O), O2 (C═O), and O3 (C−OH).

saturated 0.1 M NaOH. Reductive current was as low as 10 μA. However, at the N-doped graphene electrode (Figure 4b), the reduction peak of H_2O_2 shifted 400 mV positively with a current of 200 μA. The parallel experiments with graphene and N-plasma-treated chitosan were carried out to confirm the contribution of N doping to the high electrocatalytic activity of H_2O_2 at the N-doped graphene electrode. For the graphene-modified electrode, only a weak reduction peak was observed at −0.21 V and no obvious responses were obtained on the nitrogen-plasma-treated chitosan/GCE. The results demonstrated that the electrocatalytic activity of the graphene to H_2O_2 was mainly contributed by N doping.

Optimization of Plasma Treatment. Plasma exposure time is a key parameter to regulate the properties of the graphene in the current work because the other conditions were fixed including volume of graphene−chitosan solution for electrode modification, the power of the nitrogen plasma, the chamber pressure, and the temperature. Electrocatalytic activities of N-doped graphene with different plasma exposure times of 0, 20, 30, 40, 60, and 100 min were examined. Figure 5a is a plot of the reduction currents from cyclic voltammetric measurements of 5 mM H_2O_2 at the N-doped graphene electrode *versus* exposure time. The reduction current increased rapidly as the exposure time increased from 0 to 40 min then decreased sharply when the time was more than 40 min. According to Figure S2 (Supporting Information), the background current of the curves corresponding to 60 and 100 min were found to be much lower than those corresponding to a 40 min exposure, indicating that the longer exposure may destroy the modification film and lead to the split of the N-doped graphene film on the electrode surface. Finally, a 40 min plasma treatment was chosen as a standard preparation for N-doped graphene, and the resulting N-doped graphene electrode was used for electrochemical catalysis of H_2O_2 with the concentration ranging from 1 to 5 mM, as shown in Figure 5b. We inferred that the high level of electronic state density and the efficient quantity of free electrons in N-doped graphene facilitated H_2O_2 electrochemical reduction. As a crucial step of H_2O_2 electrocatalytic reduction, breaking of the O−O bond in H_2O_2 would become easier at the surface of N-doped graphene because N doping induced the charge delocalization of graphene. The better performance of N-doped graphene may also be ascribed to the doping effects and the change of the density of electronic states (DOEs) around the Fermi level of graphene. (1) Nitrogen atoms doped into the graphitic structure of graphene layer may form the quaternary N atoms. Because the nitrogen atom is inset into the graphite plane and bonded to three carbon atoms, quaternary N can also be described as "graphitic nitrogen" (G-N). Three
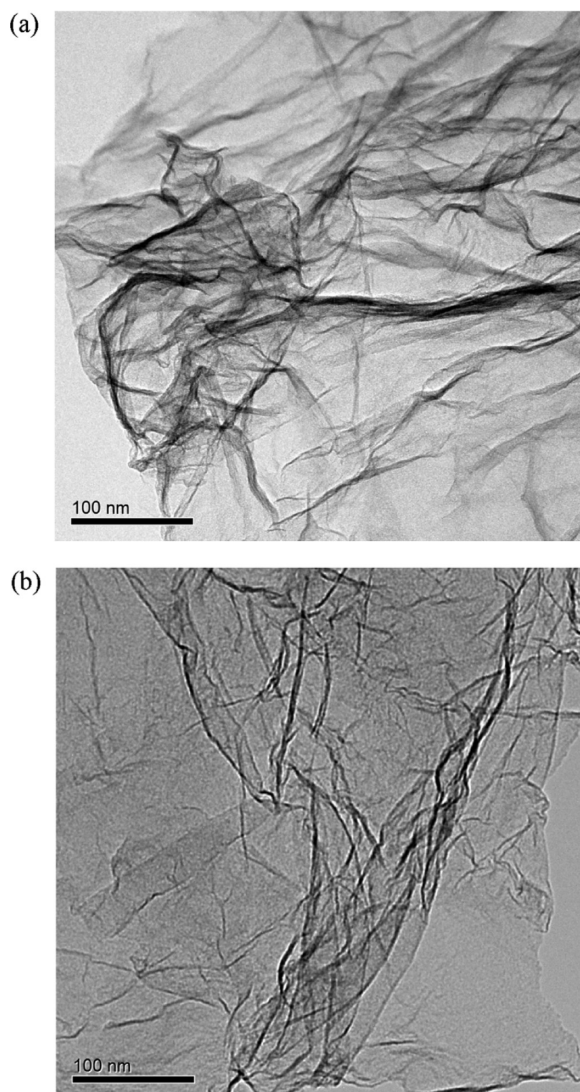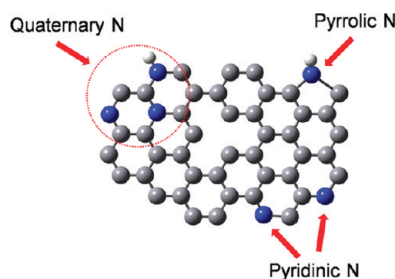

Figure 3. TEM images of graphene (a) and N-doped graphene (b).

valence electrons in G-N form σ bonds, the fourth electron fills a p-state, and the fifth electron forms a π*-state, giving the p-doping effect to N-doped graphene. (2) Nitrogen atoms doped in graphene will form pyridinic N and pyrrolic N, as shown in Scheme 1. These kinds of dopants would increase the DOEs of graphene

Scheme 1. Schematic representation of N-doped graphene. Gray for the carbon atom, blue for the nitrogen atom, and white for the hydrogen atom. A possible defect structure is shown in the middle of the ball-stick model.
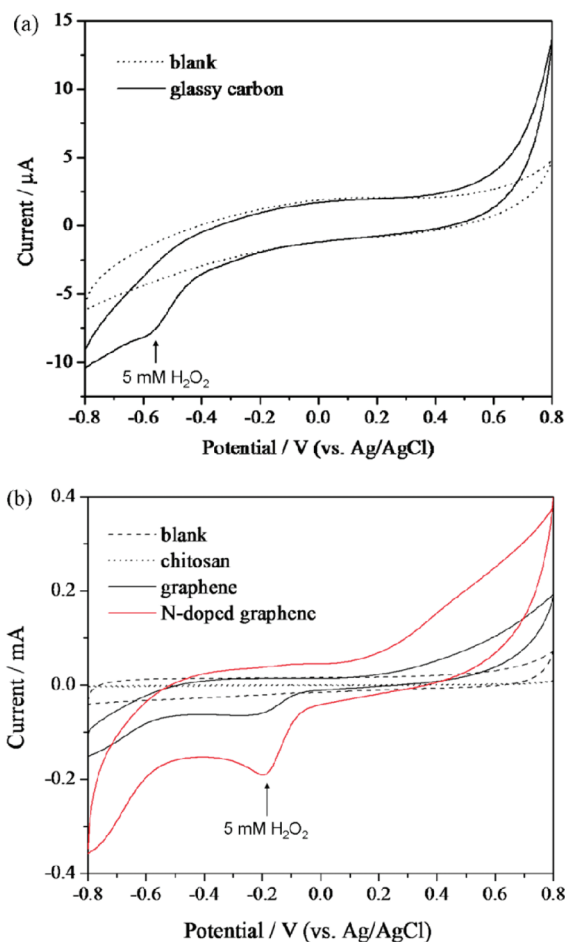
Figure 4. (a) Cyclic voltammograms of GCE in the absence (dashed line) and presence (solid line) of 5 mM H_2O_2 in N_2-saturated 0.1 M PBS (pH 7.0). (b) Cyclic voltammograms of 5 mM H_2O_2 in N_2-saturated 0.1 M PBS (pH 7.0) on chitosan electrode (dotted line), graphene electrode (black line), and N-doped graphene electrode (red line).

Figure 5. (a) Plot of the cyclic voltammetric signal (peak current) *versus* nitrogen plasma exposure time of the graphene-coated GCE (without plasma treatment and with plasma treatment of 20, 40, 60, and 100 min). (b) Cyclic voltammograms of N-doped graphene electrode in various concentration of H_2O_2 (a–g: 1, 2, 3, 4, and 5 mM) in N_2-saturated 0.1 M PBS (pH 7.0). Scan rate = 0.05 V s^{-1}.

Applications of N-Doped Graphene in Direct Electrochemistry of Glucose Oxidase and Glucose Biosensing. Glucose oxidase (GOx) was taken as a model enzyme to investigate the application of N-doped graphene in biosensing due to the leading role of GOx enzyme electrodes in glucose monitoring. GOx is a homodimer containing two tightly bound flavine adenine dinucleotide (FAD) cofactors.[49,50] Redox peaks of GOx were always hard to observe at the common electrode materials such as glassy carbon or graphite because FAD is deeply seated in a cavity and not easily accessible for direct electron transfer reaction at the electrode surface.[51,52] Herein, N-doped graphene showed its robust ability for electron transfer from the enzyme cavity to the electrode surface. Figure 6a presents the cyclic voltammograms of GOx immobilized on N-doped graphene electrode, graphene electrode, and GCE. A pair of well-defined and quasi-reversible redox peaks corresponding to the direct electrochemistry of GOx was obtained on the
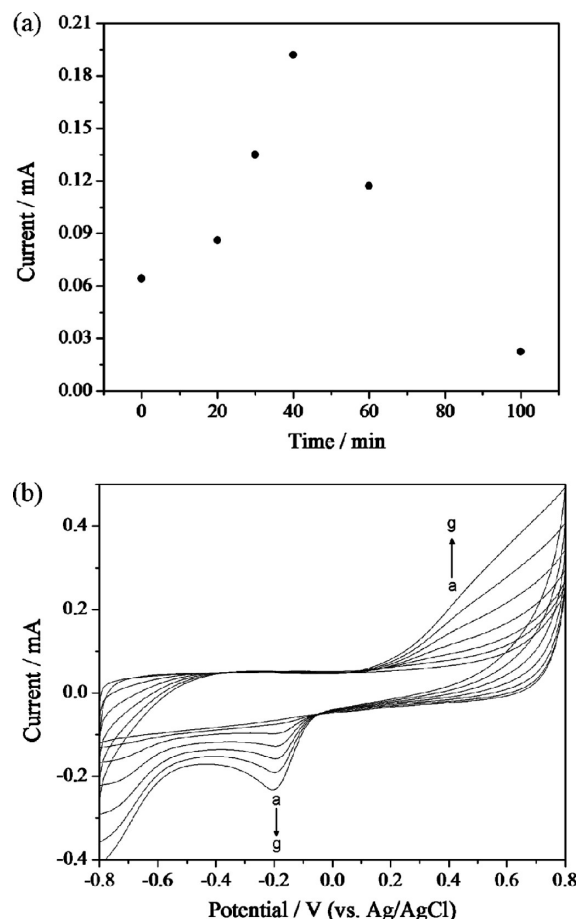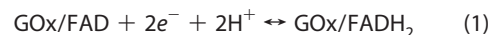
at its Fermi level and open the band gap of graphene.[46–48]

N-doped graphene electrode. Equation 1 displays the mechanism of electron transfer in GOx.

$$GOx/FAD + 2e^- + 2H^+ \leftrightarrow GOx/FADH_2 \quad (1)$$

The redox peak current is higher on N-doped graphene than on graphene because electron transfer is sensitive to the surface chemistry and DOES near the Fermi potential. By using N doping, the Fermi potential was changed and the electron transfer efficiency of N-doped graphene was enhanced. The anodic or cathodic peak currents increased linearly as the scan rate grew from 30 to 130 mV s^{-1}. Consequently, the linear relationship between anodic or cathodic peak currents and the scan rate was obtained (Figure 6b), demonstrating that the electrochemical reaction of GOx on N-doped graphene electrode is a surface-controlled process.

As we know, glucose oxidase can catalyze the oxidation of glucose with oxygen, accompanying the production of gluconic acid and H_2O_2. Consequently, glucose biosensing could be realized by detecting H_2O_2 during
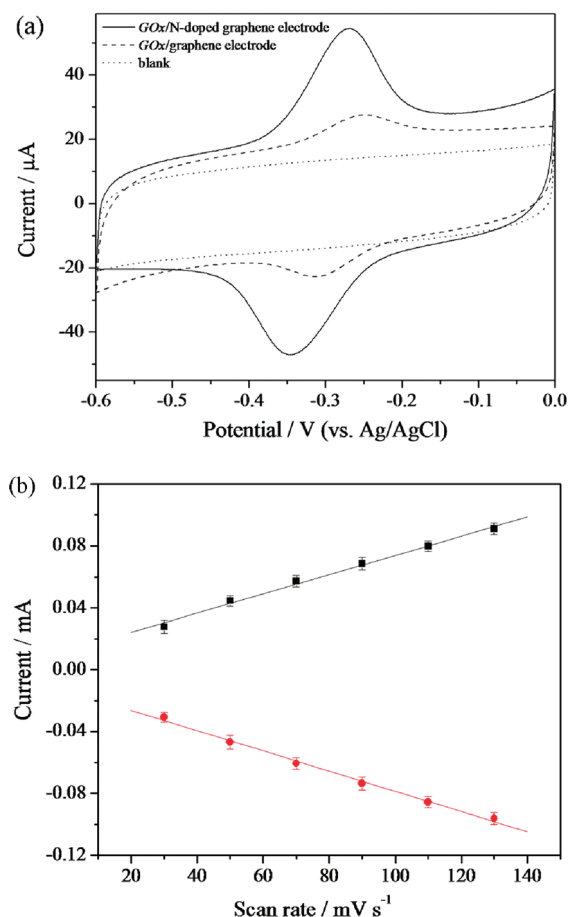
Figure 6. (a) Cyclic voltammograms of GOx immobilized on N-doped graphene electrode (solid line) and graphene electrode (dashed line) in N$_2$-saturated 0.1 M PBS solution (pH 7.0). Dotted line is for the background. Scan rate = 0.05 V s^{-1}. (b) Plot of the anodic (black line) and cathodic (red line) peak current from cyclic voltammograms of GOx immobilized on N-doped graphene electrode in N$_2$-saturated 0.1 M PBS solution (pH 7.0) *versus* different scan rate: 0.03, 0.05, 0.07, 0.09, 0.11, 0.13 V s^{-1}.

the enzymatic catalysis. Hence, the as-prepared N-doped graphene could be a promising material for glucose biosensing because it has shown the dramatic ability for H$_2$O$_2$ electrocatalysis as we described before. As shown in Figure 7a, electrochemical biosensing of glucose was realized with amperometric measurement on a N-doped graphene electrode immobilized with glucose oxidase at −0.15 V in a physiological buffer solution. Figure 7b shows the linear relationship between glucose concentration and the responding signal. The peak current increased linearly against the concentration of glucose within the range from 0.1 to 1.1 mM (*R* = 0.998). The enzymatic N-doped graphene electrode could be reused after 3 days with 4% signal lost. Experiments with interferences including ascorbic acid (AA) and uric acid (UA) were performed to test the selectivity of the N-doped graphene sensing platform. Good response to glucose ranging from 0.01 to 0.5 mM in the presence of 5 mM AA and 5 mM UA with the GOx/N-doped graphene/GCE is shown in Figure 8. Good selec-
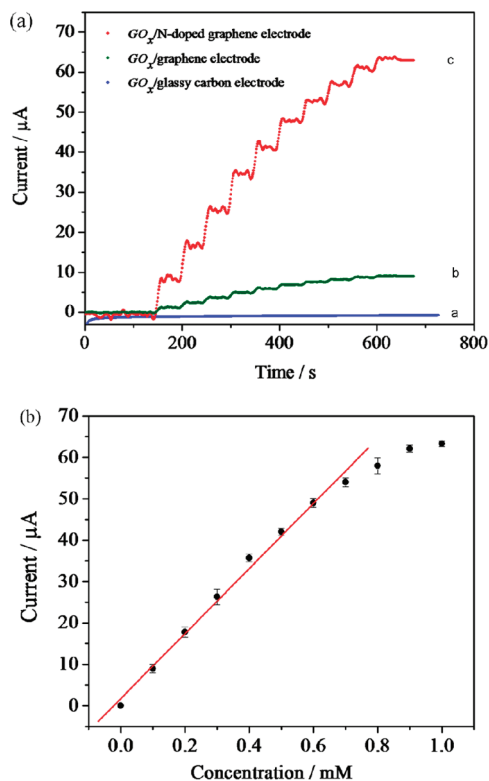

Figure 7. (a) Current−time curves for GOx immobilized on GCE (a), graphene electrode (b), and N-doped graphene electrode (c) at −0.15 V in 0.1 M PBS (pH 7.0) with successive addition of 0.1 mM glucose. (b) Calibration linear relationship for glucose with the concentration from 0.1 to 1.1 mM at N-doped graphene electrode immobilized with GOx.

tivity and sensitivity of N-doped graphene for glucose sensing suggested its potential applications as an advanced material in biosensors.

CONCLUSION

In conclusion, we have outlined a facile methodology for synthesizing N-doped graphene. Plasma treatment presents an efficient approach for simple, tunable, and fast preparation of N-doped graphene. The as-
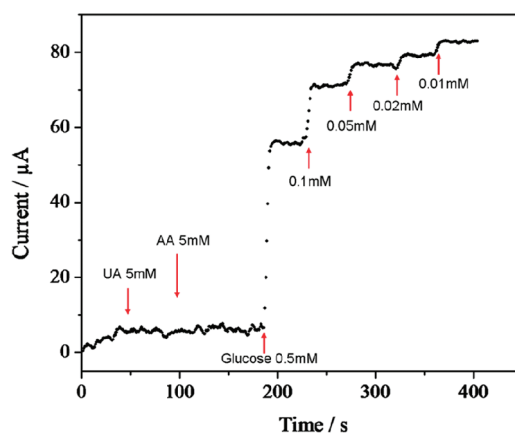

Figure 8. Chronoamperometric responses to successive addition of 5 mM uric acid, 5 mM ascorbic acid, 0.5 mM glucose, 0.1 mM glucose, 0.05 mM glucose, 0.02 mM glucose, and 0.01 mM glucose on N-doped graphene electrode immobilized with GOx at −0.15 V in 0.1 M PBS (pH 7.0).

prepared N-doped graphene exhibited excellent electrocatalytic activity for the reduction of hydrogen peroxide, fast electron transfer kinetics of glucose oxidase, and high sensitivity and selectivity for glucose biosensing. As low as 0.01 mM glucose could be detected in the presence of interferences. Moreover, since graphene has an atomic structure common to many carbon materials, doping with the plasma treatment might be an alternative method to fulfill the intrinsic modification of other carbon materials such as CNTs, graphite, carbon fiber, and porous carbon, *etc*. This work is anticipated to open a new possibility in the investigation of N-doped graphene and promote the application in addressing various electrochemical issues.

METHODS

Reagents: Graphite powder (99.9%, 325 mesh) was purchased from Alfa Aesar. Chitosan (medium molecular weight), hydrogen peroxide (50 wt % solution in water), glucose oxidase (from *Aspergillus niger*, 18200 units g^{-1}), glucose (D-(+)-99.5%), and phosphate buffered saline (PBS) were purchased from Sigma. KNO_3, $NaBH_4$, H_2SO_4, $K_2S_2O_8$, P_2O_5, $KMnO_4$, and HCl were obtained from Beijing Chemical Company. All stock solutions were prepared using deionized water without further purification.

Synthesis of Graphene: Graphite powder (2 g, 325 mesh) was put into a mixture of 12 mL of concentrated H_2SO_4, 3.0 g of $K_2S_2O_8$, and 3.0 g of P_2O_5. The solution was heated to 80 °C using an oil bath and stirred for 5 h. Next, the mixture was cooled to room temperature overnight and diluted with deionized water (500 mL). Then, the product was obtained by filtering using 0.2 μm Nylon film and dried naturally. The preoxidized graphite was then reoxidized by the Hummers and Offeman method. Pretreated graphite powder was put into 0 °C concentrated H_2SO_4 (150 mL), and 25 g of $KMnO_4$ was added gradually under stirring while the temperature of the mixture was kept around 5 °C by using an ice bath. Successively, the mixture was stirred at 35 °C for 4 h and then diluted with 250 mL of deionized water by keeping the temperature under 50 °C. One liter of water was then injected into the mixture followed by adding 30 mL of 30% H_2O_2 drop by drop. The mixture was filtered and washed with 1:10 HCl aqueous solution (1 L) to remove metal ions followed by 1 L of deionized water to remove the acid. The resulting solid was dried in air and diluted to make graphite oxide dispersion (0.5% w/w). Finally, it was purified by dialysis for 1 week to remove the remaining metal species. Exfoliation was carried out by sonicating 0.1 mg mL^{-1} graphite oxide dispersion under ambient conditions for 40 min. The resulting homogeneous yellow-brown dispersion was used for reduction. Reduction of graphene oxide was carried out by adding 5 mL of hydration hydrazine (80%) into the 50 mL solution of 0.1 mg mL^{-1} graphene oxide and kept stirring for 24 h at 80 °C. Finally, black hydrophobic powder graphene was obtained by filtrating the product and drying in vacuum.

Preparation of Nitrogen-Doped Graphene: To prepare N-doped graphene, graphene was fixed on the GCE, followed by being placed in the plasma chamber (Harrick model PDC-32G plasma cleaning unit), which was backfilled with a nitrogen atmosphere at a pressure of 750 mTorr. Plasma power was 100 W, and treatment time was 20, 40, 60, and 100 min. After nitrogen plasma treatment, N-doped graphene electrodes were thus obtained and were stored at room temperature and used directly for the electrochemical experiments.

Characterization: Transmission electron microscopy (TEM) images were obtained with a Hitachi model H-800 TEM opened at an accelerating voltage of 100 kV. XPS of the graphene oxide was obtained with a Physical Electronics Quantum 2000 scanning ESCA microprobe. AFM images were obtained with an atomic force microscope (Nanoscope III, Digital Instrument). Cyclic voltammograms (CVs) were obtained with a CHI 660a electrochemical working station (CH Instruments, Inc., USA), and amperometric measurements were made with the CHI 440a (CH Instruments, Inc., USA). A three-electrode system was employed, while the modified glassy carbon electrode (GCE, diameter 3 mm) was the working electrode, Ag/AgCl with saturated KCl solution acted as the reference electrode, and platinum wire was the counter electrode. All of the potentials in this paper were with respect to Ag/AgCl reference electrode, and the electrochemical measurements were carried out at room temperature (25 ± 2 °C). The plots for amperometric measurements are background-subtracted with the Origin 7.0 software.

Preparation of Graphene Modified Electrode and Enzyme Immobilization: The parallel electrode modified with chitosan and graphene/chitosan was prepared to carry out control experiments. Five microliters of chitosan solution (0.5 wt % with 2% acetic acid) or graphene−chitosan dispersion (1 mg mL^{-1}) was dropped onto the surface of the GCE. The GCE was precleaned by polishing with alumina powders then rinsed with ethanol and deionized water successively. The chitosan/GCE electrodes were treated with nitrogen plasma for 40 min at the power of 100 W. For the enzyme immobilization, the as-prepared N-doped graphene electrode was immersed into 10 mg mL^{-1} GOx PBS at 4 °C for 24 h, rinsed with PBS to remove the loosely adsorbed GOx, and stored at 4 °C for further measurements.

Supporting Information Available: AFM image of graphene synthesized *via* the chemical method, cyclic voltammograms of N-doped graphene electrode with different nitrogen plasma treatments, and cyclic voltammograms of N-doped graphene electrode immobilized with GOx at different scan rates. This material is available free of charge *via* the Internet at http://pubs.acs.org.

REFERENCES AND NOTES

1. Patil, A. J.; Vickery, J. L.; Scott, T. B.; Mann, S. Aqueous Stabilization and Self-Assembly of Graphene Sheets into Layered Bio-Nanocomposites Using DNA. *Adv. Mater.* **2009**, *21*, 3159–3164.
2. Lu, C. H.; Yang, H. H.; Zhu, C. L.; Chen, X.; Chen, G. N. A Graphene Platform for Sensing Biomolecules. *Angew. Chem., Int. Ed.* **2009**, *48*, 4785–4787.
3. Mohanty, N.; Berry, V. Graphene-Based Single-Bacterium Resolution Biodevice and DNA Transistor: Interfacing Graphene Derivatives with Nanoscale and Microscale Biocomponents. *Nano Lett.* **2008**, *8*, 4469–4476.
4. Wang, Y.; Lu, J.; Tang, L. H.; Chang, H. X.; Li, J. H. Graphene Oxide Amplified Electrogenerated Chemiluminescence of Quantum Dots and Its Selective Sensing for Glutathione from Thiol-Containing Compounds. *Anal. Chem.* **2009**, *81*, 9710–9715.
5. Zhou, M.; Zhai, Y. M.; Dong, S. J. Electrochemical Sensing and Biosensing Platform Based on Chemically Reduced Graphene Oxide. *Anal. Chem.* **2009**, *81*, 5603–5613.

6. Shan, C. S.; Yang, H. F.; Song, J. F.; Han, D. X.; Ivaska, A.; Niu, L. Direct Electrochemistry of Glucose Oxidase and Biosensing for Glucose Based on Graphene. *Anal. Chem.* **2009**, *81*, 2378–2382.

7. Geim, A. K.; Novoselov, K. S. The Rise of Graphene. *Nat. Mater.* **2007**, *6*, 183–191.

8. Li, X. L.; Zhang, G. Y.; Bai, X. D.; Sun, X. M.; Wang, X. R.; Wang, E.; Dai, H. J. Highly Conducting Graphene Sheets and Langmuir–Blodgett Films. *Nat. Nanotechnol.* **2008**, *3*, 538–542.

9. Shao, Y. Y.; Wang, J.; Wu, H.; Liu, J.; Aksay, I. A.; Lin, Y. H. Graphene Based Electrochemical Sensors and Biosensors. *Electroanalysis* doi: 10.1002/elan.200900571.

10. Li, Y. F.; Zhou, Z.; Shen, P. W.; Chen, Z. F. Spin Gapless Semiconductor-Metal-Half-Metal Properties in Nitrogen-Doped Zigzag Graphene Nanoribbons. *ACS Nano* **2009**, *3*, 1952–1958.

11. Ramanathan, T.; Abdala, A. A.; Stankovich, S.; Dikin, D. A.; Herrera-Alonso, M.; Piner, R. D.; Adamson, D. H.; Schniepp, H. C.; Chen, X.; Ruoff, R. S.; *et al.* Functionalized Graphene Sheets for Polymer Nanocomposites. *Nat. Nanotechnol.* **2008**, *3*, 327–331.

12. Huang, H.; Chen, S.; Gao, X. Y.; Chen, W.; Wee, A. T. S. Structural and Electronic Properties of PTCDA Thin Films on Epitaxial Graphene. *ACS Nano* **2009**, *3*, 3431–3436.

13. Boukhvalov, D. W.; Katsnelson, M. I. Chemical Functionalization of Graphene with Defects. *Nano Lett.* **2008**, *8*, 4373–4379.

14. Sundaram, R. S.; Gomez-Navarro, C.; Balasubramanian, K.; Burghard, M.; Kern, K. Electrochemical Modification of Graphene. *Adv. Mater.* **2008**, *20*, 3050–3053.

15. Vickery, J. L.; Patil, A. J.; Mann, S. Fabrication of Graphene–Polymer Nanocomposites with Higher-Order Three-Dimensional Architectures. *Adv. Mater.* **2009**, *21*, 2180–2184.

16. Guo, S. J.; Dong, S. J.; Wang, E. W. Three-Dimensional Pt-on-Pd Bimetallic Nanodendrites Supported on Graphene Nanosheet: Facile Synthesis and Used as an Advanced Nanoelectrocatalyst for Methanol Oxidation. *ACS Nano* **2010**, *4*, 547–555.

17. Sabourin, J. L.; Dabbs, D. M.; Yetter, R. A.; Dryer, F. L.; Aksay, I. A. Functionalized Graphene Sheet Colloids for Enhanced Fuel/Propellant Combustion. *ACS Nano* **2009**, *3*, 3945–3954.

18. Shao, Y. Y.; Sui, J. H.; Yin, G. P.; Gao, Y. Z. Nitrogen-Doped Carbon Nanostructures and Their Composites as Catalytic Materials for Proton Exchange Membrane Fuel Cell. *Appl. Catal. B* **2008**, *79*, 89–99.

19. Sumpter, B. G.; Meunier, V.; Romo-Herrera, J. M.; Cruz-Silva, E.; Cullen, D. A.; Terrones, H.; Smith, D. J.; Terrones, M. Nitrogen-Mediated Carbon Nanotube Growth: Diameter Reduction, Metallicity, Bundle Dispersability, and Bamboo-like Structure Formation. *ACS Nano* **2007**, *1*, 369–375.

20. Ma, Y. C.; Foster, A. S.; Krasheninnikov, A. V.; Nieminen, R. M. Nitrogen in Graphite and Carbon Nanotubes: Magnetism and Mobility. *Phys. Rev. B* **2005**, *72*, 205416.

21. Zhou, C. W.; Kong, J.; Yenilmez, E.; Dai, H. J. Modulated Chemical Doping of Individual Carbon Nanotubes. *Science* **2000**, *290*, 1552–1555.

22. Wehling, T. O.; Novoselov, K. S.; Morozov, S. V.; Vdovin, E. E.; Katsnelson, M. I.; Geim, A. K.; Lichtenstein, A. I. Molecular Doping of Graphene. *Nano Lett.* **2008**, *8*, 173–177.

23. Chen, W.; Chen, S.; Qi, D. C.; Gao, X. Y.; Wee, A. T. S. Surface Transfer p-Type Doping of Epitaxial Graphene. *J. Am. Chem. Soc.* **2007**, *129*, 10418–10422.

24. Liu, L.; Ryu, S. M.; Tomasik, M. R.; Stolyarova, E.; Jung, N.; Hybertsen, M. S.; Steigerwald, M. L.; Brus, L. E.; Flynn, G. W. Graphene Oxidation: Thickness-Dependent Etching and Strong Chemical Doping. *Nano Lett.* **2008**, *8*, 1965–1970.

25. Giovannetti, G.; Khomyakov, P. A.; Brocks, G.; Karpan, V. M.; van den Brink, J.; Kelly, P. J. Doping Graphene with Metal Contacts. *Phys. Rev. Lett.* **2008**, *101*, 026803.

26. Lee, S. U.; Belosludov, R. V.; Mizuseki, H.; Kawazoe, Y. Designing Nanogadgetry for Nanoelectronic Devices with Nitrogen-Doped Capped Carbon Nanotubes. *Small* **2009**, *5*, 1769–1775.

27. Jang, J. W.; Lee, C. E.; Lyu, S. C.; Lee, T. J.; Lee, C. J. Structural Study of Nitrogen-Doping Effects in Bamboo-Shaped Multiwalled Carbon Nanotubes. *Appl. Phys. Lett.* **2004**, *84*, 2877–2879.

28. Ivanovskaya, V. V.; Zobelli, A.; Stephan, O.; Briddon, P. R.; Colliex, C. BN Domains Included into Carbon Nanotubes: Role of Interface. *J. Phys. Chem. C* **2009**, *113*, 16603–16609.

29. Panchalkarla, L. S.; Govindaraj, A.; Rao, C. N. R. Nitrogen- and Boron-Doped Double-Walled Carbon Nanotubes. *ACS Nano* **2007**, *1*, 494–500.

30. Deng, S. Y.; Jian, G. Q.; Lei, J. P.; Hu, Z.; Ju, H. X. A Glucose Biosensor Based on Direct Electrochemistry of Glucose Oxidase Immobilized on Nitrogen-Doped Carbon Nanotubes. *Biosens. Bioelectron.* **2009**, *25*, 373–377.

31. Carrero-Sanchez, J. C.; Elias, A. L.; Mancilla, R.; Arrellin, G.; Terrones, H.; Laclette, J. P.; Terrones, M. Biocompatibility and Toxicological Studies of Carbon Nanotubes Doped with Nitrogen. *Nano Lett.* **2006**, *6*, 1609–1616.

32. Wang, X. R.; Li, X. L.; Zhang, L.; Yoon, Y.; Weber, P. K.; Wang, H. L.; Guo, J.; Dai, H. J. N-Doping of Graphene through Electrothermal Reactions with Ammonia. *Science* **2009**, *324*, 768–771.

33. Wei, D. C.; Liu, Y. Q.; Wang, Y.; Zhang, H. L.; Huang, L. P.; Yu, G. Synthesis of N-Doped Graphene by Chemical Vapor Deposition and Its Electrical Properties. *Nano Lett.* **2009**, *9*, 1752–1758.

34. Chen, Q. D.; Dai, L. M.; Gao, M.; Huang, S. M.; Mau, A. Plasma Activation of Carbon Nanotubes for Chemical Modification. *J. Phys. Chem. B* **2001**, *105*, 618–622.

35. Hummers, W. S.; Offeman, R. E. Preparation of Graphitic Oxide. *J. Am. Chem. Soc.* **1958**, *80*, 1339.

36. Xia, J. L.; Chen, F.; Li, J. H.; Tao, N. J. Measurement of the Quantum Capacitance of Graphene. *Nat. Nanotechnol.* **2009**, *4*, 505–509.

37. Wang, Y.; Li, Y. M.; Tang, L. H.; Lu, J.; Li, J. H. Application of Graphene Modified Electrode for Selective Detection of Dopamine. *Electrochem. Commun.* **2009**, *11*, 889–892.

38. Yang, D.; Velamakanni, A.; Bozoklu, G.; Park, S.; Stoller, M.; Piner, R. D.; Stankovich, S.; Jung, I.; Field, D. A.; Ventrice, C. A.; *et al.* Chemical Analysis of Graphene Oxide Films after Heat and Chemical Treatments by X-ray Photoelectron and Micro-Raman Spectroscopy. *Carbon* **2009**, *47*, 145–152.

39. Matter, P. H.; Zhang, L.; Ozkan, U. S. The Role of Nanostructure in Nitrogen-Containing Carbon Catalysts for the Oxygen Reduction Reaction. *J. Catal.* **2006**, *239*, 83–96.

40. Jansen, R. J. J.; Vanbekkum, H. XPS of Nitrogen-Containing Functional-Groups on Activated Carbon. *Carbon* **1995**, *33*, 1021–1027.

41. Nakayama, Y.; Soeda, F.; Ishitani, A. XPS Study of the Carbon–Fiber Matrix Interface. *Carbon* **1990**, *28*, 21–26.

42. Malitesta, C.; Losito, I.; Sabbatini, L.; Zambonin, P. G. New Findings on Polypyrrole Chemical Structure by XPS Coupled to Chemical Derivatization Labelling. *J. Electron Spectrosc. Relat. Phenom.* **1995**, *76*, 629–634.

43. Niwa, Y.; Kobayash; H; Tsuchiya, T. X-ray Photoelectron-Spectroscopy of Tetraphenylporphin and Phthalocyanine. *J. Chem. Phys.* **1974**, *60*, 799–807.

44. Brisson, P. Y.; Darmstadt, H.; Fafard, M.; Adnot, A.; Servant, G.; Soucy, G. X-ray Photoelectron Spectroscopy Study of Sodium Reactions in Carbon Cathode Blocks of Aluminium Oxide Reduction Cells. *Carbon* **2006**, *44*, 1438–1447.

45. Veal, E. A.; Day, A. M.; Morgan, B. A. Hydrogen Peroxide Sensing and Signaling. *Mol. Cell* **2007**, *26*, 1–14.

46. Yang, S. H.; Shin, W. H.; Kang, J. K. The Nature of Graphite- and Pyridinelike Nitrogen Configurations in Carbon Nitride Nanotubes: Dependence on Diameter and Helicity. *Small* **2008**, *4*, 437–441.

47. Saha, S. K.; Chandrakanth, R. C.; Krishnamurthy, H. R.; Waghmare, U. V. Mechanisms of Molecular Doping of Graphene: A First-Principles Study. *Phys. Rev. B* **2009**, *80*, 155414.

48. Biel, B.; Blase, X.; Triozon, F.; Roche, S. Anomalous Doping Effects on Charge Transport in Graphene Nanoribbons. *Phys. Rev. Lett.* **2009**, *102*, 096803.

49. Lin, Y. H.; Lu, F.; Tu, Y.; Ren, Z. F. Glucose Biosensors Based on Carbon Nanotube Nanoelectrode Ensembles. *Nano Lett.* **2004**, *4*, 191–195.

50. Wang, J. Electrochemical Glucose Biosensors. *Chem. Rev.* **2008**, *108*, 814–825.

51. Kang, X.; Wang, J.; Wu, H.; Aksay, I. A.; Liu, J.; Lin, Y. Glucose Oxidase−Graphene−Chitosan Modified Electrode for Direct Electrochemistry and Glucose Sensing. *Biosens. Bioelectron.* **2009**, *25*, 901–905.

52. Zhang, X.; Wang, J.; Ogorevc, B.; Spichiger, U. E. Glucose Nanosensor Based on Prussian-Blue Modified Carbon−Fiber Cone Nanoelectrode and an Integrated Reference Electrode. *Electroanalysis* **1999**, *11*, 945–949.